JOURNAL OF GEOPHYSICAL RESEARCH, VOL. 114, A02222, doi:10.1029/2008JA013647, 2009

Hybrid simulations of magnetic reconnection initiated in the magnetosheath

N. Omidi,[1] T. Phan,[2] and D. G. Sibeck[3]

Received 29 July 2008; revised 13 October 2008; accepted 2 December 2008; published 26 February 2009.

[1] Interaction of solar wind tangential discontinuities (TDs) with the bow shock may initiate reconnection in the magnetosheath. We employ 2.5-D electromagnetic, hybrid simulations that treat the ions kinetically via particle-in-cell methods and the electrons as a massless fluid to study this interaction. We present results from eight runs corresponding to TD thicknesses ranging from 10 to 260 ion skin depths and shear angles ranging from 120° to 180°. Our results indicate a transition from time-dependent to steady state reconnection as the thickness of the solar wind TD increases above 30 ion skin depths. As the shear angle in the magnetic field decreases, it takes longer to initiate reconnection, and reconnection jet speeds diminish, suggesting a lower reconnection rate. Implications of these results for magnetic reconnection at currents sheets in general and at the magnetopause in particular are also discussed.

Citation: Omidi, N., T. Phan, and D. G. Sibeck (2009), Hybrid simulations of magnetic reconnection initiated in the magnetosheath, *J. Geophys. Res.*, *114*, A02222, doi:10.1029/2008JA013647.

1. Introduction

[2] The interaction of the time varying solar wind and its embedded discontinuities with the bow shock is a complex process resulting in a variety of phenomena depending on the properties of the discontinuities and the geometry of the shock. This interaction may involve the formation of multiple discontinuities predicted by fluid theory [e.g., *Neubauer*, 1975] or kinetic structures such as hot flow anomalies (HFAs) [e.g., *Schwartz et al.*, 1988; *Paschmann et al.*, 1988].

[3] Another type of interaction, previously identified by *Lin* [1997] and *Maynard et al.* [2001, 2002] using hybrid and global MHD simulations, respectively, is the initiation of magnetic reconnection in the magnetosheath at TDs accompanied by rotations in the IMF direction. *Phan et al.* [2007] recently reported observational evidence for this kind of interaction. Using ACE observations, they noted the presence of a TD with thickness of about 260 ion skin depths in the solar wind. At a later time, corresponding to the arrival of this discontinuity into the magnetosheath, the Cluster spacecraft detected a much thinner (about 12 ion skin depths) discontinuity. In addition to a smaller width, the discontinuity was found to be associated with reconnection jets. *Phan et al.* [2007] concluded that the thick discontinuity in the solar wind was compressed by the bow shock triggering magnetic reconnection in the sheath.

[4] The occurrence of magnetic reconnection in the magnetosheath raises a number of important questions regarding its global consequences for the magnetosphere and ionosphere as discussed by *Maynard et al.* [2002]. It also provides a great opportunity to investigate properties of magnetic reconnection in a relatively simple configuration (e.g., nearly symmetric plasmas on both sides of the discontinuity) without feedback from distant boundary conditions, such as the ionosphere in studies of magnetospheric reconnection. Observations of magnetic reconnection in the solar wind [e.g., *Gosling et al.*, 2005, 2006; *Phan et al.*, 2006] and magnetosheath provide many new opportunities to examine this important process in a new regime of parameter space and learn about its general characteristics.

[5] The objectives of this paper focus on the properties of reconnection in the magnetosheath and not its global magnetospheric consequences which require much longer simulation runs. Accordingly, we use 2.5-D global hybrid (kinetic ions, fluid electrons) simulations to investigate the interaction of TDs with the bow shock and how the internal structure of the TDs determines properties of magnetosheath reconnection. The use of hybrid simulations allows us to investigate this interaction on ion temporal and spatial scales such as gyrofrequency, gyroradii and skin depth. In addition, the bow shock in these simulations includes ion dissipation processes and the associated ULF waves in a self-consistent manner allowing us to investigate their impact on the TD interactions and magnetic reconnection. Specifically, we concentrate on the impact of discontinuity thickness and magnetic shear on the time dependence and efficiency of reconnection. The organization of the paper is as follows. In section 2, we describe the model used for the study, while in section 3 we describe results from runs with different TD thicknesses and magnetic shears. We also compare the structure of a reconnection layer in a simulation run with that reported by *Phan et al.* [2007]. Section 4

[1]Solana Scientific Incorporated, Solana Beach, California, USA.
[2]Space Sciences Laboratory, University of California, Berkeley, California, USA.
[3]NASA Goddard Space Flight Center, Greenbelt, Maryland, USA.

0148-0227/09/2008JA013647$09.00

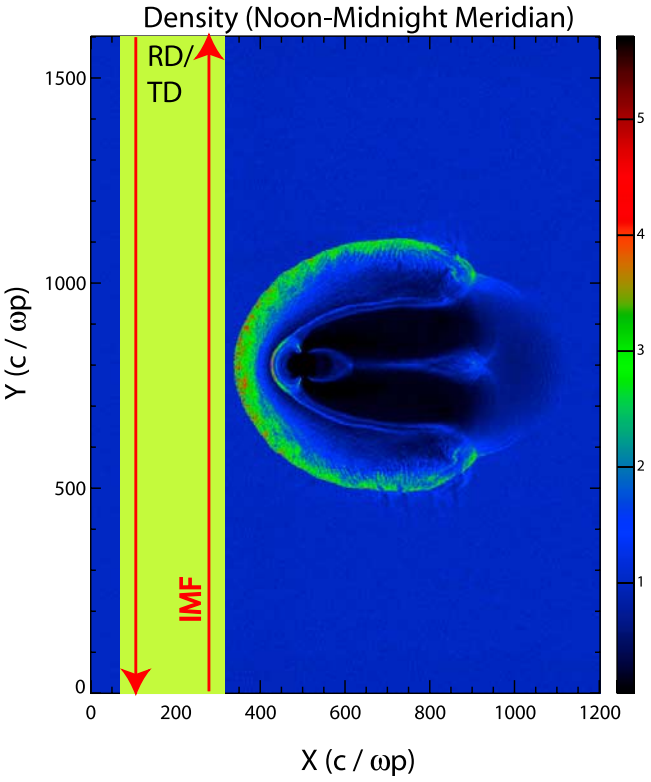

Figure 1. Color intensity plot of plasma density in the simulation box illustrates the bow shock and magnetosphere and the TD upstream of them. TD normal is along the X direction.

provides the summary and conclusions of the study and their implications for reconnection at the magnetopause.

2. Hybrid Simulation Model

[6] The main tool of investigation is a 2.5-D (2-D in space and 3-D in currents and electromagnetic fields) global hybrid simulation used extensively in recent years [e.g., *Omidi et al.*, 2004, 2005; *Omidi and Sibeck*, 2007]. In electromagnetic hybrid codes, ions are treated as macroparticles and consist of one or more species (e.g., differing mass, charge, etc.) whereas electrons are treated as a massless, charge neutralizing fluid [see, e.g., *Winske and Omidi*, 1993, 1996]. The details of the global hybrid model are described in the work of *Omidi et al.* [2005] and only a brief description is given here. Figure 1 illustrates the model used in this study. The simulation plane corresponds to the X-Y plane with X along the solar wind flow direction (Sun-Earth line) and Y pointing along the dipole axis. Thus, the X and Y directions in the simulations correspond to −X and Z axes, respectively in the GSM coordinate system. Consequently, the X-Y simulation plane corresponds to the noon-midnight meridional plane with Y pointing northward. The simulation box extends 1200 ion skin depths (c/ω_p, where c is the speed of light and ω_p is the ion plasma frequency) in the X direction and 1600 in the Y direction with cell size of 1 ion skin depth. The solar wind Alfven Mach number is 5 and the electron and ion betas (ratio of kinetic to magnetic pressure) are each set to 0.5.

[7] The IMF initially lies in the X-Y plane, points northward (+Y) and makes a 90° angle with the *x* axis. We use this initial IMF orientation to generate the bow shock (and magnetosphere) shown in Figure 1. The tangential discontinuity is placed in the solar wind upstream of the bow shock with normal along the *x* axis. Table 1 shows the properties of the eight TDs used in this study. The thickness of these TDs varies between 10 and 260 ion skin depth in the solar wind. The IMF never has any component along the *x* axis as required for TDs in the Y-Z plane. The shear angle noted in Table 1 corresponds to the angle of IMF with respect to the *y* axis measured in the counter clockwise direction so that a shear angle of 180° corresponds to a southward IMF and 120° corresponds to a negative By and positive Bz. Also, in Table 1 the thickness of the TDs in the magnetosheath at the subsolar point are shown. Except for run 2 for a TD with linear polarization, the remaining runs have TDs with circular polarization. Neither the magnetic field strength, nor any of the other plasma parameters change across the discontinuity. In the remainder of the paper, we use the configuration in Figure 1 as the beginning of time and only refer to time beyond this point.

[8] A constant resistivity corresponding to a resistive length scale of 1/3 ion skin depth is used throughout the simulation domain in all the runs. As a result, the contribution of the resistive term to the electric field through the generalized Ohm's law and its variations in the simulation domain is controlled by the current density. This is desirable in that the question of where and when reconnection occurs is controlled by the dynamics and evolution of the current layer. Thus, we can examine the role of TD structure in the reconnection process keeping the role of resistivity the same in all cases. We should also note that while the size of the simulated magnetosphere is comparable to that of Mercury (i.e., smaller than Earth's) the results presented here are applicable over a wide range of scales. This is because the simulated bow shock and magnetosheath are not sensitive to the size of the system as long as it is much larger than ion kinetic scales [see, e.g., *Omidi et al.*, 2004, 2005; *Blanco-Cano et al.*, 2006a; *Omidi and Sibeck*, 2007].

3. Description of the Results

3.1. Steady State and Time-Dependent Reconnection

[9] The simulation results indicate that the thickness of TDs directly controls the time dependence of reconnection. To illustrate this point we begin by describing the results of runs 1 and 2 in Table 1. Figure 2 shows a close-up of the density around the dayside bow shock and magnetosheath at time Ω t = 100 (Ω is the ion gyrofrequency) from run 1. Also shown in Figure 2 are a number of open magnetic field lines on either side of the TD as well as closed magnetospheric field lines. The magnetic field loops in the magnetosheath indicate that the interaction of the TD with the bow shock has resulted in magnetic reconnection between open field lines in the magnetosheath. This is further illustrated in Figure 3 which shows ion velocity in the Y direction. Comparisons between Figures 2 and 3 show enhanced northward and southward plasma acceleration within the region of reconnected (looped) magnetic field lines. Throughout this study, we use the presence of accelerated flows within the TD layer as an indication of magnetic

Table 1. TD Thickness in Solar Wind and Sheath, As Well As Magnetic Shear Angle and Polarization of TDs in the Eight Runs Described

Run	TD Thickness in Solar Wind (Ion Skin Depth)	Shear Angle (deg)	Polarization	TD Thickness in Sheath (Ion Skin Depth)
1	260	180	circular	14
2	10	180	linear	5
3	10	180	circular	5
4	30	180	circular	12
5	10	150	circular	4
6	10	120	circular	7
7	30	150	circular	9
8	30	120	circular	12

reconnection. Note that upstream of the TD in the Southern Hemisphere, Figure 3 shows northward (green) moving plasma. This plasma originates as a result of formation of a transitory solitary shock [see *Omidi and Sibeck*, 2007] during the passage of the TD through the Southern Hemisphere bow shock. Acceleration of this northward moving plasma by reconnection leads to southward flow within the reconnection layer with speeds comparable to that in the magnetosheath further upstream. The formation of the solitary shock is due to the B_Z associated with the polarization of the TD (i.e., B_Z within the rotation layer). This is why the solitary shock is transitory in nature. We should also note that a change in the sign of B_Z (i.e., polarization of TD) would have resulted in the formation of the solitary shock in the Northern Hemisphere.

[10] Figure 4 shows a cut along the trajectory L1 in Figure 3. The top two panels show the Y and Z components of the magnetic field normalized to solar wind values. The finite value of Bz within the rotation layer is due to the circular polarization of the TD. As indicated in Table 1, the initial width of the TD was 260 ion skin depths while Figure 4 shows the reconnection layer to have a width of 12 ion skin depths. Thus, as the TD crosses the shock its thickness is reduced, which implies the current density in the sheet is enhanced until reconnection is initiated. In other words, reconnection is due to the compression of the TD by the bow shock. Because of its broad width, it took 45 ion gyroperiods for the TD to go through the subsolar shock while magnetic reconnection started at Ω t = 65 (see Table 2). The third panel in Figure 4 shows the density

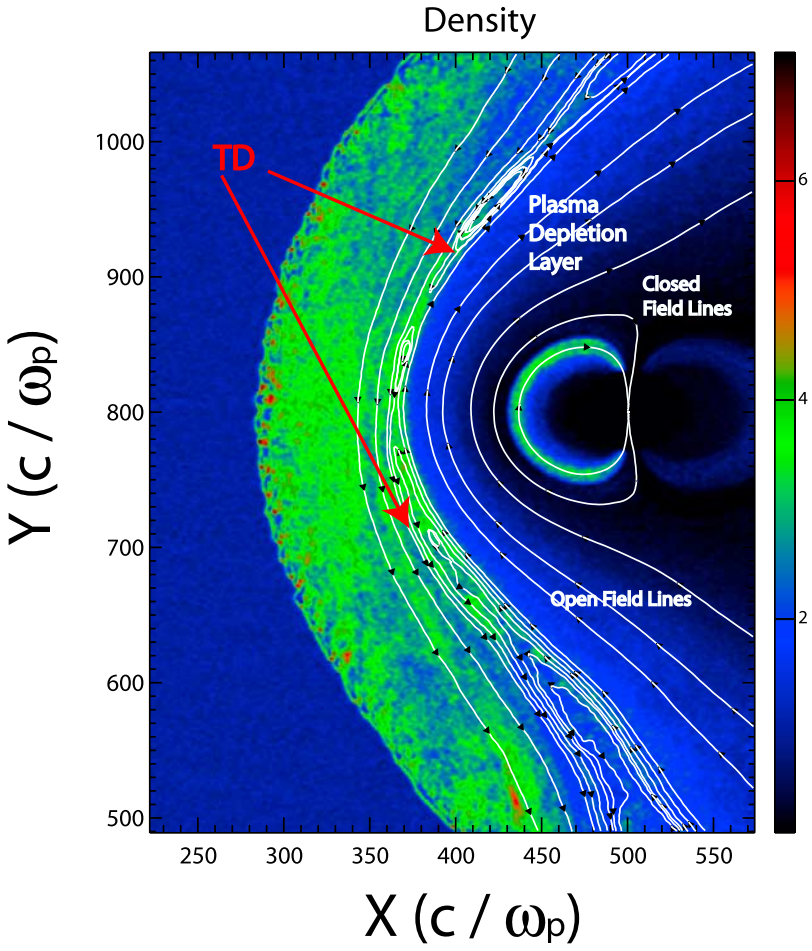

Figure 2. Color intensity plot of density zoomed around dayside bow shock and magnetopause at Ω t = 100. Also shown are magnetic field lines illustrating magnetic reconnection between open fields in the sheath.

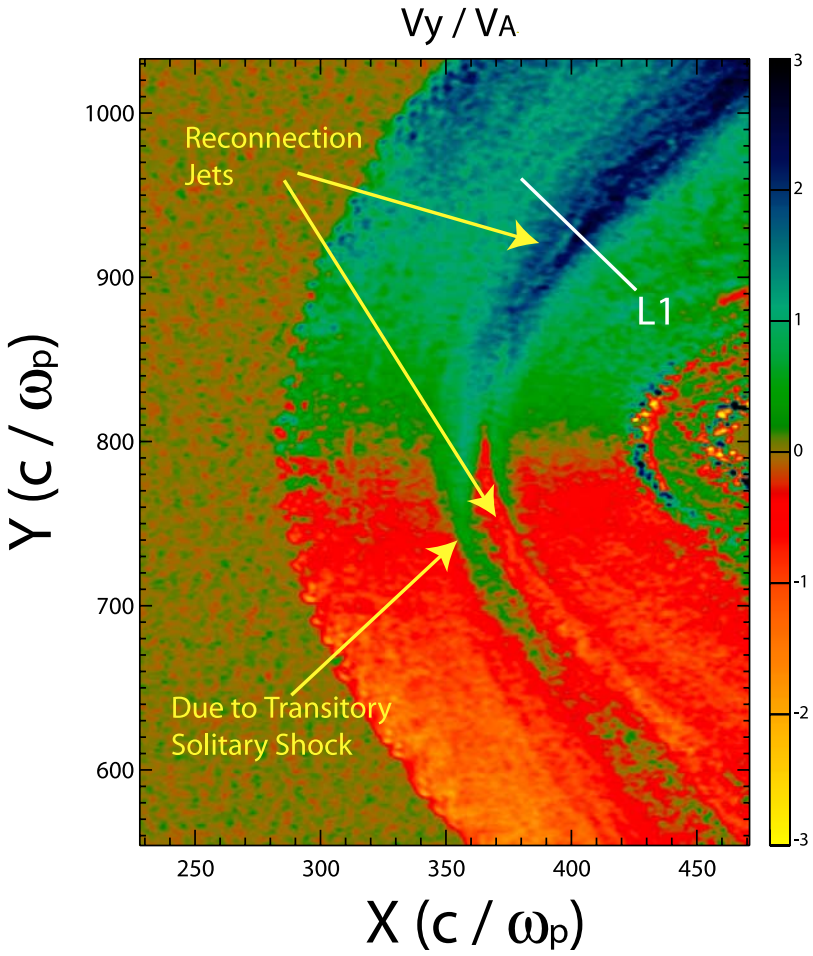

Figure 3. Ion flow velocity in the Y direction illustrates reconnection jets in both hemispheres in run 1. Owing to the relatively uniform nature of jets, reconnection is identified to be in steady state.

normalized to its solar wind value. As a result of TD compression, density is enhanced within the reconnection layer. Also, evident is a drop in density across the TD. The fourth panel in Figure 4 shows the Y component of ion flow velocity which shows plasma acceleration associated with reconnection. The bottom panel shows magnetic field strength normalized to IMF strength, illustrating a drop within the reconnection layer and a jump across the TD. We should note that cuts along different paths through the TD show characteristics similar to those in Figure 4, although the details vary. The results described here indicate that run 1 corresponds to quasi-steady reconnection although some time variability is present as discussed later.

[11] Figure 5 shows the Y component of ion flow velocity associated with run 2 for a much thinner solar wind TD. In contrast to Figure 3, the reconnection jets in Figure 5 exhibit a spatial structure resulting from time-dependent reconnection. To examine the time-dependent reconnection, Figures 6 and 7show snapshots of the current density in the Z direction and the magnetic field lines. The two panels in Figure 6 correspond to Ω t = 12.5 and 25, i.e., times shortly after the passage of the TD through the shock. As indicated in Table 2, it took only 6.5 ion gyroperiods for the TD to cross the nose of the bow shock. The passage of the TD through the shock is associated with the formation of many small magnetic islands shown in Figure 6. The spatial scales of these islands is of the order of a few ion skin depths and is comparable to the wavelength of the waves (mirror and ion cyclotron) generated at and downstream of the bow shock in association with ion dissipation [*Winske and Quest*, 1988; *McKean et al.*, 1994; Blanco-Cano et al. 2006a, 2006b] and the shock surface waves [*Burgess and Scholer*, 2007]. This suggests that, the evolution and dynamics of the current sheet are impacted significantly by the presence of these waves through localized and multiple thinning and intensification of the current density. A comparison of the two panels in Figure 6 shows that the magnetic islands coalesce into larger structures. Continuation of this trend is clearly evident in the two panels in Figure 7 which correspond to Ω t = 50 and 75. While the formation of magnetic islands and their coalescence to longer wavelengths is reminiscent of the ion tearing instability, we can rule out this instability as the initiator of reconnection. This is due to the fact that parts of the current sheet that do not interact with the bow shock do not undergo reconnection. In other words, the TDs initiated in this study are not tearing unstable and interaction with the shock is essential for reconnection to occur. On the other hand, once

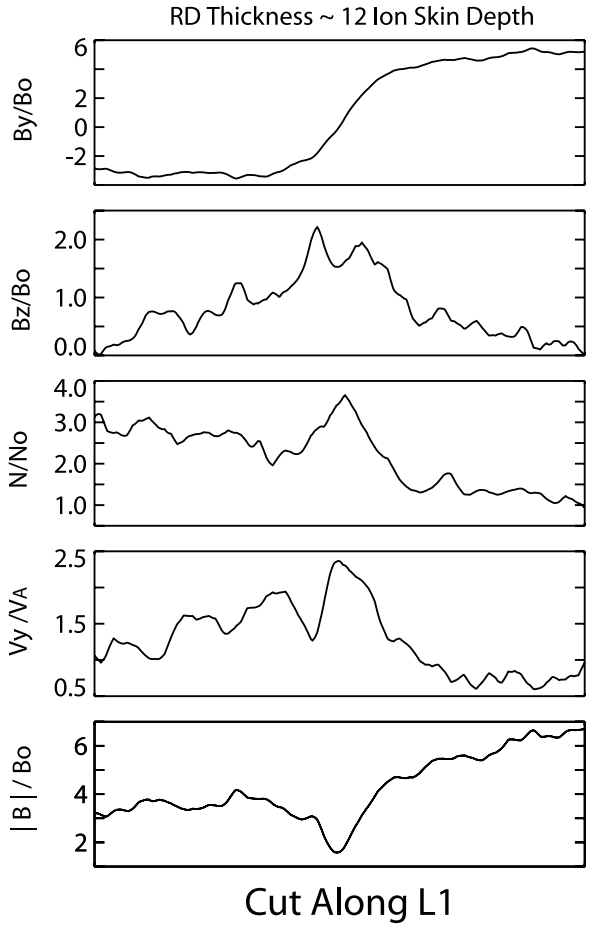

Figure 4. Plasma and field parameters along the trajectory L1 in Figure 3 are shown. See section 3.1 for description.

the magnetic islands have formed we cannot rule out a connection between the coalescence observed in this study and that associated with the nonlinear evolution of the tearing instability.

[12] In addition to being thinner, the TD in run 2 is linearly polarized, possibly causing the time dependency of reconnection in this run. This possibility was ruled out by performing run 3 which is similar to 2 except that the TD has a circular polarization. It was found that the results from these two runs are very similar, indicating that the time-dependent reconnection results from the thin TD. By increasing the TD thickness to 30 ion skin depths in run 4, we find that the resulting reconnection is no longer time-dependent (i.e., no islands form). Accordingly, TDs with thicknesses beyond a few 10s of ion skin depth lead to quasi-steady reconnection in the magnetosheath.

3.2. Antiparallel and Component Reconnection

[13] The TDs in runs 1 through 4 correspond to magnetic shear angles of 180°, i.e., antiparallel reconnection. In runs 5 through 8 we examine the effects of shear angles less than 180°, corresponding to component merging. In addition, we use runs 5–8 to further confirm the earlier conclusion regarding the role of TD thickness on time-dependent reconnection. Specifically, in runs 5 and 6 the TD thickness is 10 and the shear angles are 150° and 120°, respectively, while in runs 7 and 8 the TD thickness is 30 with the same shear angles. As indicated in Table 2, TDs with thicknesses of 10 ion skin depths exhibit time-dependent reconnection regardless of the shear angle while TDs with thicknesses of 30 exhibit steady state reconnection.

[14] To compare the efficiency of the reconnection process in runs 1–8, Table 2 shows the time it took for reconnection to initiate and also, the change in magneto-sheath flow speed associated with the reconnection jets. It is evident that the thicker the TD, the longer it takes for reconnection to start. This behavior is consistent with shock compression causing the reconnection process. Also, for a given TD thickness the smaller the shear angle the longer it takes for reconnection to initiate. The reconnection flow speed in Table 2 is normalized to the local Alfven speed using the antiparallel component of the magnetic field strength. In the classical definition of magnetic reconnection rate, it is assumed that the out flow speed is Alfvenic and therefore, only the inflow speed is used in calculating the reconnection rate. It is evident in Table 2, however that the outflow speeds vary from Alfvenic to sub-Alfvenic between the 8 runs. Specifically, for a given TD thickness the jet speed decreases with decreasing shear angle. We interpret this decrease in outflow jet speed as being due to a smaller reconnection rate in that the rate of flux removal decreases with decreasing jet speed. Comparing the jet speeds in runs 2, 3, 5 and 6 it is evident the efficiency of reconnection decreases with decreasing shear angle. The results of runs 4, 7 and 8 further support these conclusions.

3.3. Comparison With Cluster Observations

[15] Among the 8 TDs considered in this study, the one associated with run 1 most resembles the thick TD observed by *Phan et al.* [2007] in the solar wind. In the remainder of this section we compare the plasma and magnetic field signatures associated with the reconnection layer observed in Cluster data with those seen in run 1. We should emphasize that the solar wind conditions in run 1 are similar but not identical to those during the *Phan et al.* [2007] event. Similarly, the TD structure in run 1 is not identical to that in the observations and for example, it has the opposite polarization (rotation of the magnetic field). As a result, we would expect the transitory solitary shock to have formed in the Northern Hemisphere during the *Phan et al.* [2007] event where Cluster was in the Southern Hemisphere (see *Omidi and Sibeck* [2007] for details on solitary shocks).

Table 2. T1, T2, and Time Dependency of Reconnection and Reconnection Jet Speed for the Eight Runs in Table 1[a]

Run	T1 (Ω^{-1})	T2 (Ω^{-1})	Steady Reconnection	Reconnection Flow Speed (V_A)
1	45	65	yes	0.5
2	6.5	18	no	1.0
3	6.5	18	no	1.0
4	8	18	yes	0.8
5	6.5	28	no	0.9
6	6.5	44	no	0.6
7	8	40	yes	0.27
8	8	55	yes	0.25

[a]T1, time after launch for TD to cross subsolar bow shock; T2, time for magnetic reconnection to initiate; V_A, local Alfven speed.

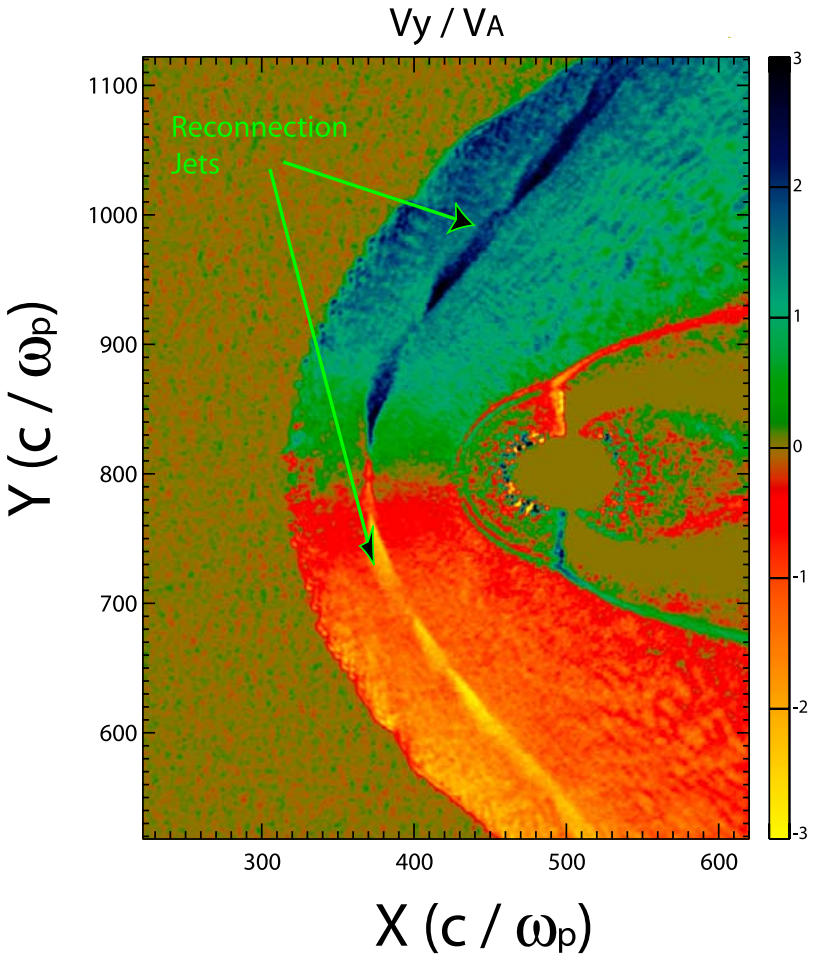

Figure 5. The same as in Figure 3 except for run 2. Owing to the spatially nonuniform nature of jets, reconnection is identified to be time-dependent.

Although Cluster was in the Southern Hemisphere, it was located north of the reconnection site and observed flows in the northward direction. To accommodate the comparison between run 1 and Cluster data, the simulation data has been modified in a number of ways. Specifically, they were transformed into GSE coordinates and given real values for density, velocity and magnetic field (as opposed to using normalized values) by using simultaneously observed solar wind plasma and field values. Strictly speaking the use of these values is not consistent with the solar wind conditions used in run 1 but for our purposes it suffices. The left panels in Figure 8 show the GSE Z component of the magnetic field, plasma density, Z component of ion velocity and the total field strength from run 1 while the right hand panels show the corresponding data from Cluster [*Phan et al.*, 2007]. The cut associated with this profile was made in the Northern Hemisphere. As part of the transformation of the simulation date, the sense of rotation of B_{ZGSE} in the left panel has been changed to agree with that in the Cluster data.

[16] The comparison of simulation results with observations reveals many similarities. First, the thicknesses of the TDs in the magnetosheath are similar, indicating similar levels of compression undergone by the both observed and simulated TDs. Second, the simulation accurately predicts the density enhancement within the reconnection layer and the overall drop in density across the TD. Third, the simulation predicts the depressed magnetic field strength within the reconnection layer, and a decrease (but not the observed reversal) in the north/south flow velocity. We emphasize that this general agreement between the simulation results and observations is not tied to the exact cut used in the left panel in Figure 8 but would apply to any cut across the simulated TD which would show the same general characteristics. Our classification of reconnection in run 1, as steady state is supported by the relative uniformity of the reconnection jets in Figure 3 in contrast to the spatially varying jet speeds in Figure 5. We should note however, that there are time variations in the position of the reconnection line and at times more than one X-line is present along the current sheet. This suggests that some level of time dependency is inherent to the reconnection process and one can only compare and contrast general properties of the reconnection layer. We discuss this point in more detail in the next section.

4. Summary and Conclusions

[17] We presented results from global hybrid simulations that address the interaction of TDs with the bow shock and

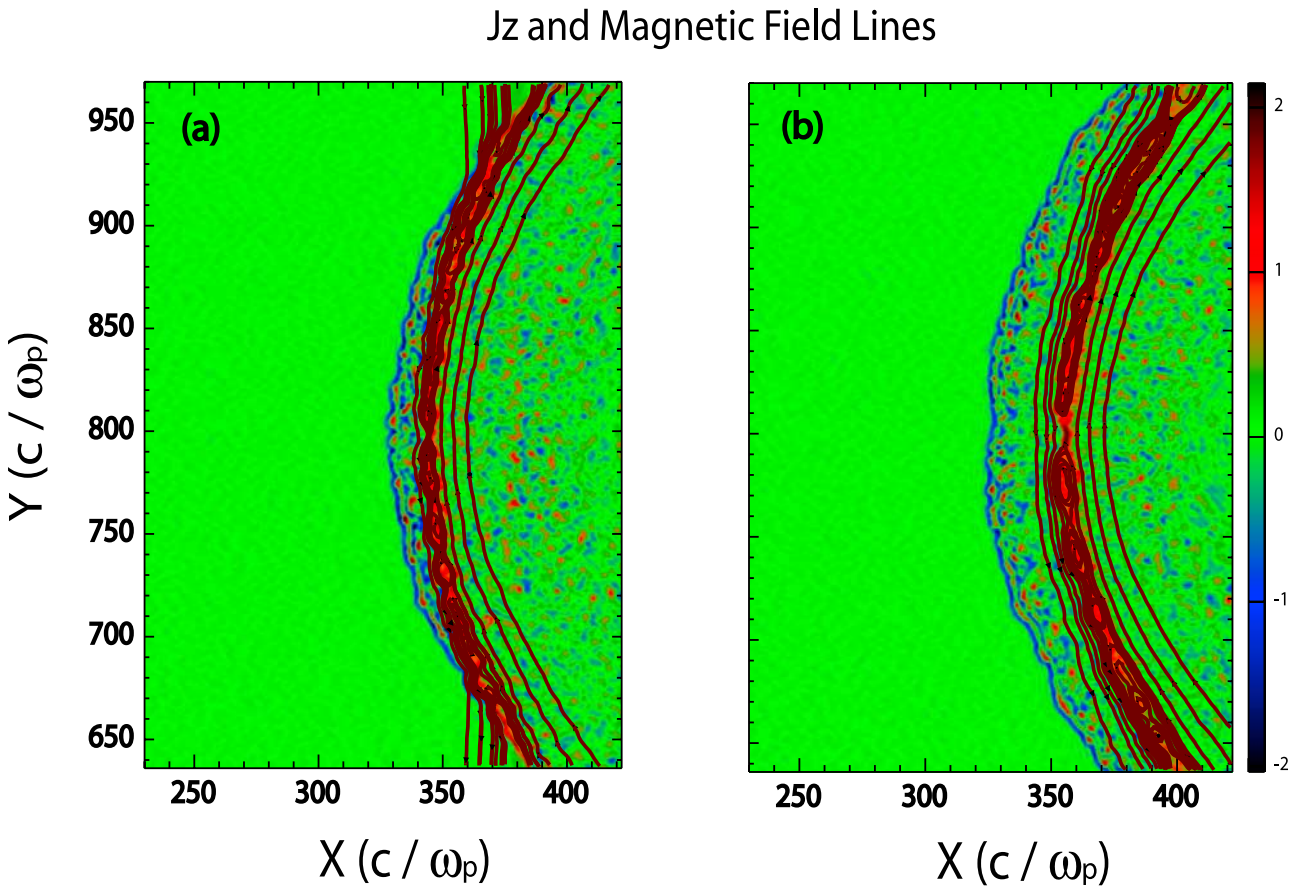

Figure 6. Color intensity plots of current density in the Z direction and magnetic field lines zoomed around the bow shock. The formation of magnetic island structures at the TDs is evident.

the ensuing magnetic reconnection in the magnetosheath. Using TDs of various thickness, polarization, and magnetic shear angle a number of conclusions are reached. One is that the thickness of the TD determines whether reconnection in the magnetosheath is steady state or time-dependent with the latter occurring when TD thickness is $\sim<$ 10–20 ion skin depth. The other is that both steady state and time-dependent reconnection occur for magnetic shear angles at or less than 180° implying the occurrence of both antiparallel and component merging. The results demonstrate that as the shear angle decreases it takes longer for reconnection to initiate and also the reconnection rate is reduced. It is also found that polarization of the TD does not impact the nature of reconnection in the sheath.

[18] This study supports earlier conclusions reached regarding the importance of shock compression in the initiation of magnetic reconnection in the magnetosheath [*Maynard et al.*, 2001, 2002; *Phan et al.*, 2007]. The results also show that depending on the thickness of the TD, shock compression can lead to the initiation of time steady or dependent reconnection. When the thickness of the TD is comparable to the wavelengths of the surface waves at the bow shock and compressional waves downstream of it, the interaction results in the formation of a large number of magnetic islands and x-line-like structures. These structures are not initially associated with plasma acceleration, but with time they coalesce to larger islands and reconnection jets develop. Figures 6 and 7 clearly illustrate the continued formation of larger islands owing to coalescence of smaller ones, i.e., a transition from smaller to larger wavelengths. Examination of the current sheet's evolution with time also shows a reverse process namely the formation of small islands in the vicinity of the x-lines as the current sheet thickness decreases locally to a few ion skin depths. This thinning process is associated with the intensification of the current density and its eventual bifurcation, yet another manifestation of island formation. This thinning and bifurcation process introduces an inherent time dependency to the reconnection process so that even when it seems to be in steady state with uniform reconnection jets, the current sheet thickness and the position of the x-line do vary with time.

[19] While the results presented here are relevant to all current sheets in general, here we examine their implications for the magnetopause which is exposed to similar types of ULF waves and turbulence as the TDs considered here. Some of the most important and outstanding questions regarding reconnection at the magnetopause are related to whether it occurs in a steady state or time-dependent fashion and whether it corresponds to antiparallel or component merging. Considering the results presented here, one would conclude that both time-dependent and steady state recon-

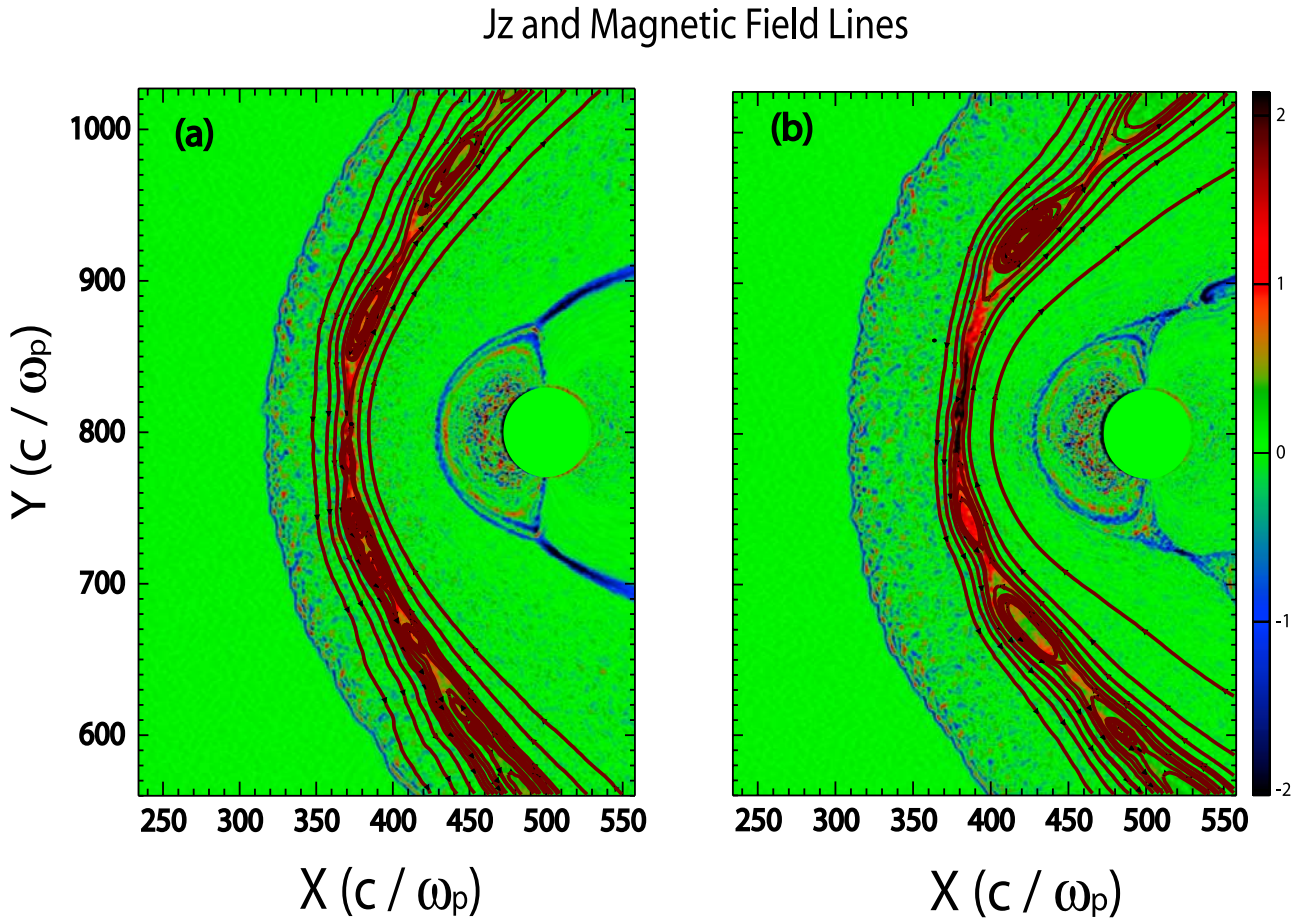

Figure 7. The same as in Figure 6 except at later times and a broader zoom containing the dayside magnetopause. Formation of larger islands owing to coalescence of smaller ones is illustrated.

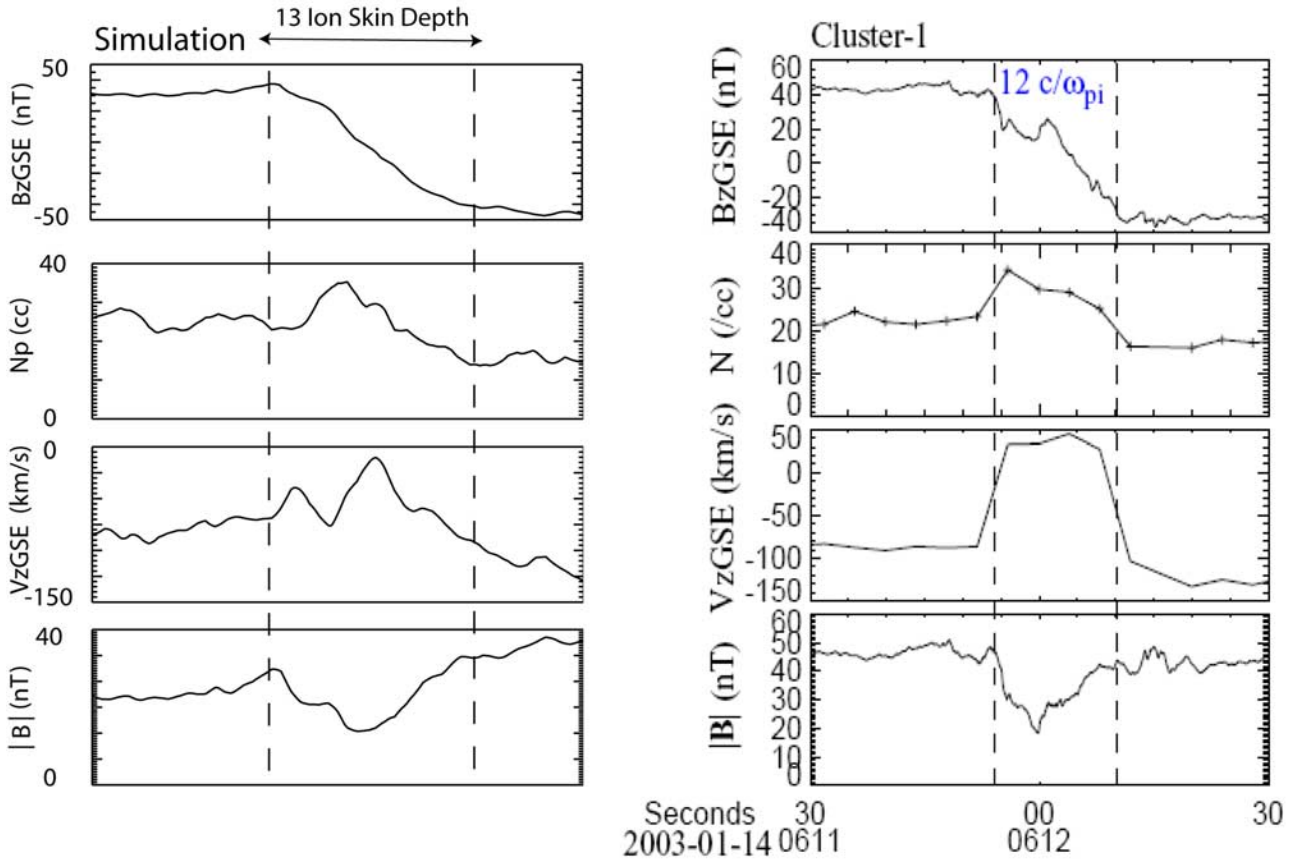

Figure 8. Plasma and field parameters from simulation run 1 (left panels) and Cluster spacecraft in the magnetosheath (right panels).

nection occur at the magnetopause with the thickness of the current sheet as the main indicator. Be it due to external forcing (e.g., a pressure pulse in the magnetosheath), or as part of the current sheet evolution, the thickness of the magnetopause varies in space and time. At times and places where the current sheet is thin, the ensuing reconnection is expected to be time-dependent while it would be closer to steady state when the magnetopause thickness is larger than 10–20 ion skin depth.

[20] The results presented here also indicate that component merging is possible. Our finding that reconnection occurs fastest and at its highest rate for antiparallel geometries suggests that the rate of reconnection cannot be uniform along reconnection lines with both antiparallel and component merging geometries. Nor would we expect the simultaneous initiation of reconnection along extended lines at the magnetopause.

[21] **Acknowledgments.** Work for this project was supported by NSF grant ATM-0502992 to Solana Scientific Inc. Work by D. G. Sibeck was funded by RTOP 955518.02.01.02.29, Dynamics of the Bow Shock.

[22] Amitava Bhattacharjee thanks the reviewers for their assistance in evaluating manuscript this paper.

References

Blanco-Cano, X., N. Omidi, and C. T. Russell (2006a), Macrostructure of collisionless shocks: 2. ULF waves in the foreshock and magnetosheath, *J. Geophys. Res.*, *111*, A10205, doi:10.1029/2005JA011421.

Blanco-Cano, X., N. Omidi, and C. T. Russell (2006b), ULF waves and their influence on bow shock and magnetosheath structures, *Adv. Space Res.*, *37*, 1522, doi:10.1016/j.asr.2005.10.043.

Burgess, D., and M. Scholer (2007), Shock front instability associated with reflected ions at perpendicular shock, *Phys. Plasmas*, *14*, 012108, doi:10.1063/1.2435317.

Gosling, J. T., R. M. Skoug, D. J. McComas, and C. W. Smith (2005), Direct evidence for magnetic reconnection in the solar wind near 1 AU, *J. Geophys. Res.*, *110*, A01107, doi:10.1029/2004JA010809.

Gosling, J. T., S. Eriksson, R. Skoug, D. McComas, and R. Forsyth (2006), Petschek-type reconnection exhausts in the solar wind well beyond 1 AU: Ulysses, *Astrophys. J.*, *644*, 613, doi:10.1086/503544.

Lin, Y. (1997), Generation of anomalous flows near the bow shock by its interaction with interplanetary discontinuities, *J. Geophys. Res.*, *102*, 24265, doi:10.1029/97JA01989.

Maynard, N. C., W. Burke, P. Sandholt, J. Moen, D. Ober, M. Lester, D. Wiemer, and A. Egeland (2001), Observations of simultaneous effects of merging in both hemispheres, *J. Geophys. Res.*, *106*, 24,551, doi:10.1029/2000JA000315.

Maynard, N. C., et al. (2002), Predictions of magnetosheath merging between IMF field lines of opposite polarity, *J. Geophys. Res.*, *107*(A12), 1456, doi:10.1029/2002JA009289.

McKean, M. E., D. Winske, and S. P. Gary (1994), Two-dimensional simulations of ion anisotropy instabilities in the magnetosheath, *J. Geophys. Res.*, *99*, 11,141, doi:10.1029/93JA03025.

Neubauer, F. M. (1975), Nonlinear oblique interaction of interplanetary discontinuities with magnetogasdynamic shocks, *J. Geophys. Res.*, *80*, 1213, doi:10.1029/JA080i010p01213.

Omidi, N., and D. Sibeck (2007), Formation of hot flow anomalies and solitary shocks, *J. Geophys. Res.*, *112*, A01203, doi:10.1029/2006JA011663.

Omidi, N., X. Blanco-Cano, C. Russell, and H. Karimabadi (2004), Dipolar magnetospheres and their characterization as a function of magnetic moment, *Adv. Space Res.*, *33*(11), 1996.

Omidi, N., X. Blanco-Cano, and C. T. Russell (2005), Macro-structure of collisionless bow shocks: 1. Scale lengths, *J. Geophys. Res.*, *110*, A12212, doi:10.1029/2005JA011169.

Paschmann, G., G. Haerendel, N. Sckopke, E. Mobius, H. Luhr, and C. Carlson (1988), Three-dimensional plasma structures with anoma-

lous flow directions near the Earth's bow shock, *J. Geophys. Res.*, *93*, 11,279, doi:10.1029/JA093iA10p11279.

Phan, T. D., et al. (2006), A Magnetic reconnection x-line extending more than 390 Earth radii in the solar wind, *Nature*, *439*, 175, doi:10.1038/nature04393.

Phan, T. D., G. Paschmann, C. Twitty, F. Mozer, J. Gosling, J. Eastwood, M. Oieroset, H. Reme, and E. Lucek (2007), Evidence for magnetic reconnection initiated in the magnetosheath, *Geophys. Res. Lett.*, *34*, L14104, doi:10.1029/2007GL030343.

Schwartz, S. J., R. Kessel, C. Brown, L. Woolliscroft, M. Dunlop, C. Farrugia, and D. Hall (1988), An active current sheet near the Earth's bow shock, *J. Geophys. Res.*, *93*, 11,295, doi:10.1029/JA093iA10p11295.

Winske, D., and N. Omidi (1993), Hybrid codes: Methods and applications, in *Computer Space Plasma Physics: Simulation Techniques and Software*, edited by H. Matsumoto and Y. Omura, p. 103, Terra Sci., Tokyo.

Winske, D., and N. Omidi (1996), A nonspecialist's guide to kinetic simulations of space plasmas, *J. Geophys. Res.*, *101*, 17,287, doi:10.1029/96JA00982.

Winske, D., and K. B. Quest (1988), Magnetic field and density fluctuations at perpendicular supercritical collisionless shocks, *J. Geophys. Res.*, *93*, 9681, doi:10.1029/JA093iA09p09681.

N. Omidi, Solana Scientific Incorporated, 777 South Pacific Coast Highway, 208, Solana Beach, CA 92075, USA. (omidi@solanasci.com)

T. Phan, Space Sciences Laboratory, University of California, Berkeley, CA 94720, USA.

D. G. Sibeck, NASA Goddard Space Flight Center, Code 674, 8800 Greenbelt Road, Greenbelt, MD 20771, USA.